CHAPTER 4

SIMULATION RESULTS AND DISCUSSIONS

In the course of the development of the model applied to a single column PSA system with a phenomena of pressure drop occuring within the column and not available in the literature the starting point was Sundaram and Wankat's 1988 paper entitled "pressure drop effects in the pressurization and blowdown steps of pressure swing adsorption" [5]. In that paper they presented a mathematical analysis of only a pressurization step and a blowdown step with no integration between both steps, and no products being produced. The second reference communication which forms the basis of this study was US patent 4,194,892 fielded in 1980 by Jones, Keller,and Wells entitled "Rapid pressure swing adsorption process with high enrichment factor" [1]. The patent was a very qualitative one and difficult to use for design purpose. This study was aimed at developing a model that could be used to explain some of the behavior of single column PSA systems as found in the patent using design concepts of the first paper.

The following will present the development and simulation of the model and the points of discussions raised.

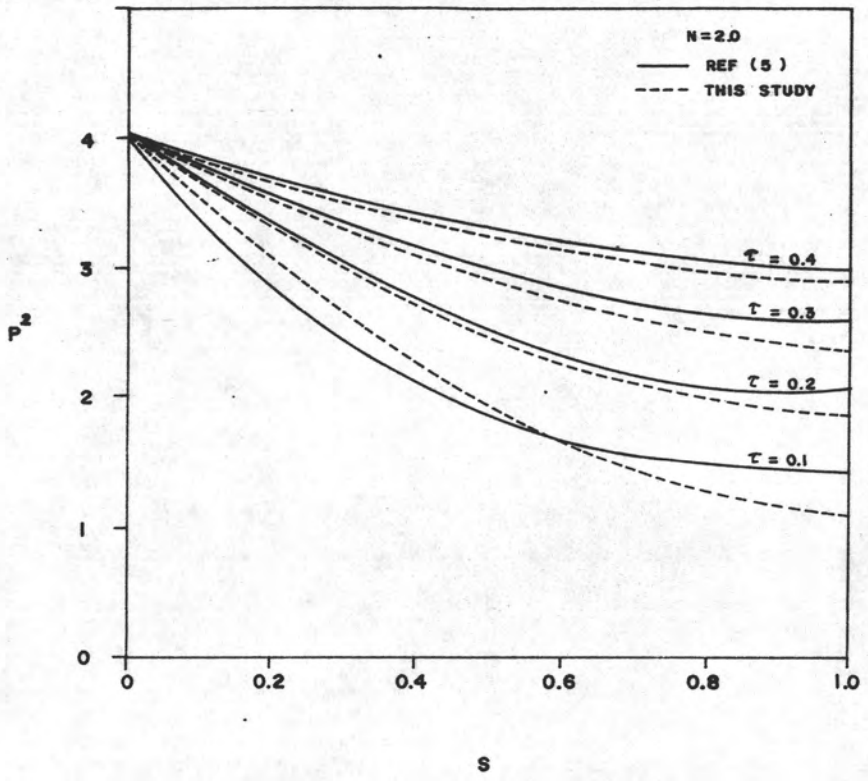

Figure 4.1 Comparison between pressurization step the Sundaram and Wankat system with this system with V_s approaching zero.

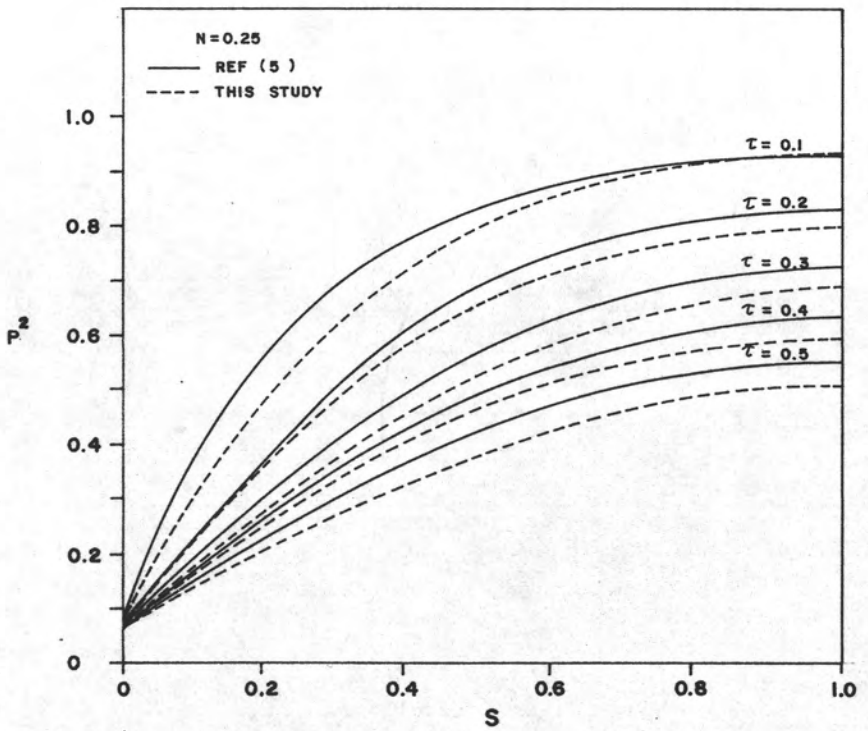

Figure 4.2 Comparison between blowdown step the Sundaram and Wankat system with this system with V_s approaching zero.

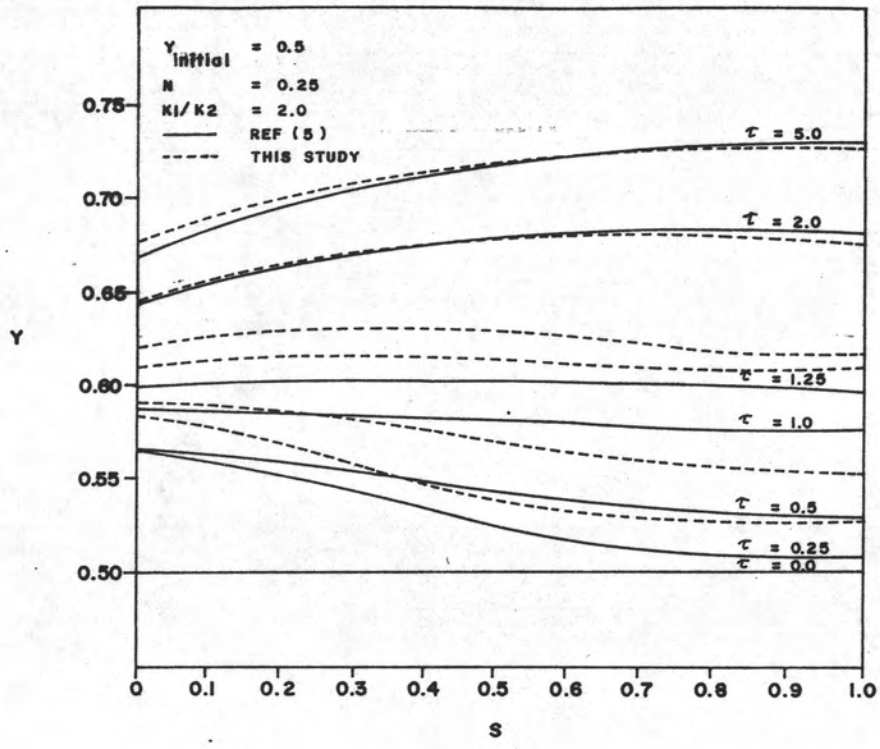

Figure 4.3 Comparison of concentration profile from this simulation and from Sundaram and Wankat simulation at blowdown.

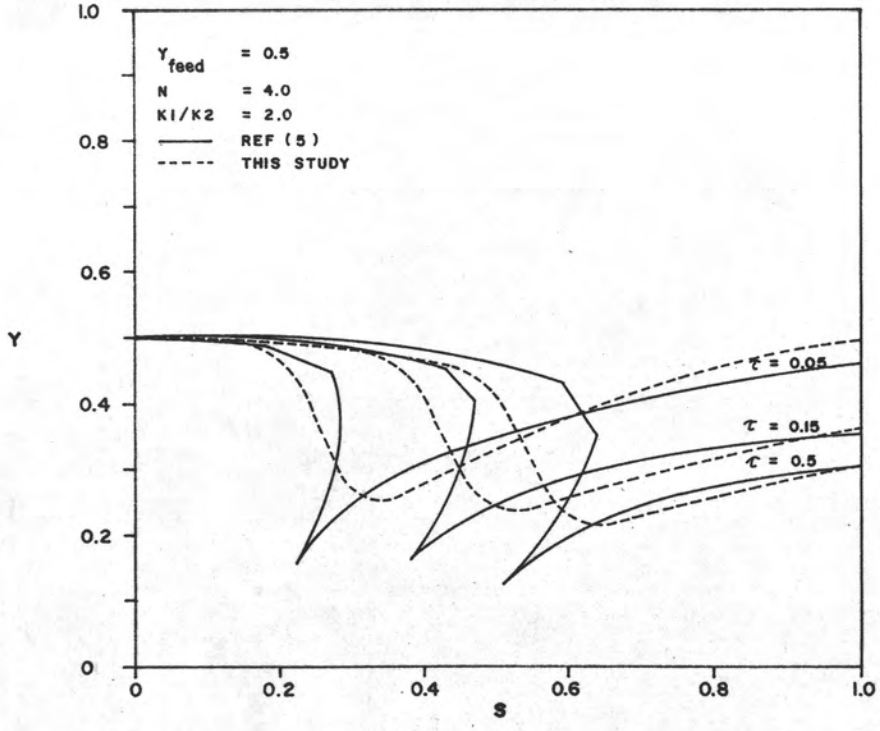

Figure 4.4 Comparison of concentration profile from this simulation and from Sundaram and Wankat simulation at pressurization.

4.1 Comparative study of the model developed in this study with the model proposed by Sundaram and Wankat .

The geometry of Sundaram and Wanket's system was a single adsorption bed (152.4 cm long) and their simulation consisted on one hand in pressurizing the system from the front end of the column while maintaining the back end of the column closed and observing the pressure profiles as a function of time, and on the other hand in depressurizing the column by rapidly opening a valve at the front end of the column and maintaining the back end of the column closed and again observing the depressurization profiles for pressure as a function of time.

The system in this study was a little bit more complicated in that in our study the adsorption column is linked to a product surge tank. In the Jones patent one of the column used was 150 cm long and the product surge tank volume to empty adsorption column had a ratio of 1 to 3 (this is the ratio used in this study) . In this study the column simulated was 150 cm in length, an inside diameter of 7.52 cm and a product surge tank volume of V_s=2250 cm^3.

For pressurization and blowdown simulations Sundaram and Wankat make use of the following equations

$$[K_1-y(K_1-K_2)]\frac{\partial y}{\partial t} + v\frac{\partial y}{\partial z} + \frac{y(1-y)(K_1-K_2)}{p}\frac{\partial p}{\partial t} = 0 \qquad (3.21)$$

$$\frac{\partial}{\partial z}\left[\frac{vp}{K_2} + \frac{(K_1-K_2)vpy}{K_1K_2}\right] = -C\frac{\partial^2 p^2}{\partial z^2} \qquad (3.24)$$

for pressurization the I.C. is $p(z,t=0) = p_L$, $y(z,t=0) = y_{feed}$ and B.C.'s $p(z=0,t) = p_H$; $\partial p(L,t)/\partial z = 0$; $y(z=0,t) = y_{feed}$; for blowdown the I.C. is $p(z,t=0) = p_H$, $y(z,t=0) = y_{initial}$ and B.C.'s $p(z=0,t) = p_L$; $\partial p(L,t)/\partial z = 0$

In the analysis made in this study equations 3.21 and 3.24 are also used but the boundary conditions are different for pressurization. In particular we have an additional term for the boundary between adsorbent bed and product surge tank as presented before in equation 3.32

$$v(L,t)p(L,t)A\varepsilon = V_s \frac{\partial p(L,t)}{\partial t} + ERT \qquad (3.32)$$

and for pressurization the I.C.'s will be the same as above. The B.C.'s will be $p(z=0,t) = p_H$, $y(z=0,t) = y_{feed}$, and for blowdown the I.C.'s will be the same as above the B.C.'s will be $p(z=0,t) = p_L$, $y(z=L,t) = y_C$ where V_s is the volume of the product surge tank.

In order to have some sort of comparison between both sets of equations the boundary conditions which include the surge tank volume, term V_s was made as small as possible and E equal to zero so that the physical system of this study approaches the Sundaram and Wankat system. Sundaram and Wankat used a $y_{initial}$ of 0.5 and dimensionless terms τ , S and N where

$$\tau = \frac{\varepsilon^3 d_p^2 p_0 t}{150(1-\varepsilon)^2 \mu l^2} \quad , S = z/L \quad , N = p_f/p_0$$

p_f is the final pressure and p_0 is the initial pressure of the

bed. From the term N we have N<1 for the blowdown step and N>1 for the pressurization step, where y is the mole fraction of more strongly adsorbed component.

As comparison is presented in figure 4.1 for the pressurization step and figure 4.2 for the blowdown step. As shown in figure 4.1 a comparison of P^2 as a function of dimensionless bed length indicates compatibility with the simulation results of Sundaram and Wankat for τ = 0.2 -0.4 but for τ =0.1 there are some deviations. And for the blowdown step as shown in figure 4.2 the compatibility is comparable.

For the next comparison we simulated conditions at blowdown for y_{intial} =0.5 , N = 0.25 and K_1/K_2 =2.0 . The results as shown in figure 4.3 with mole fraction as a function of column length show good agreement in the trends of the curves although the exact values are not exactly the same .

Furthermore, we simulated a pressurization step at y_{feed}=0.5 N =4.0 and K_1/K_2 = 2.0. The results as shown in figure 4.4 show mole fraction as a function of column length . The trends of the results are similar and include a shock wave as mentioned in Sundaram and Wankat although the exact profiles differ. The difference could be explained by the different methods used to solve the equations.

Generally it can then be said that this simulation follows the trend of Sundaram and Wankat fairly well.

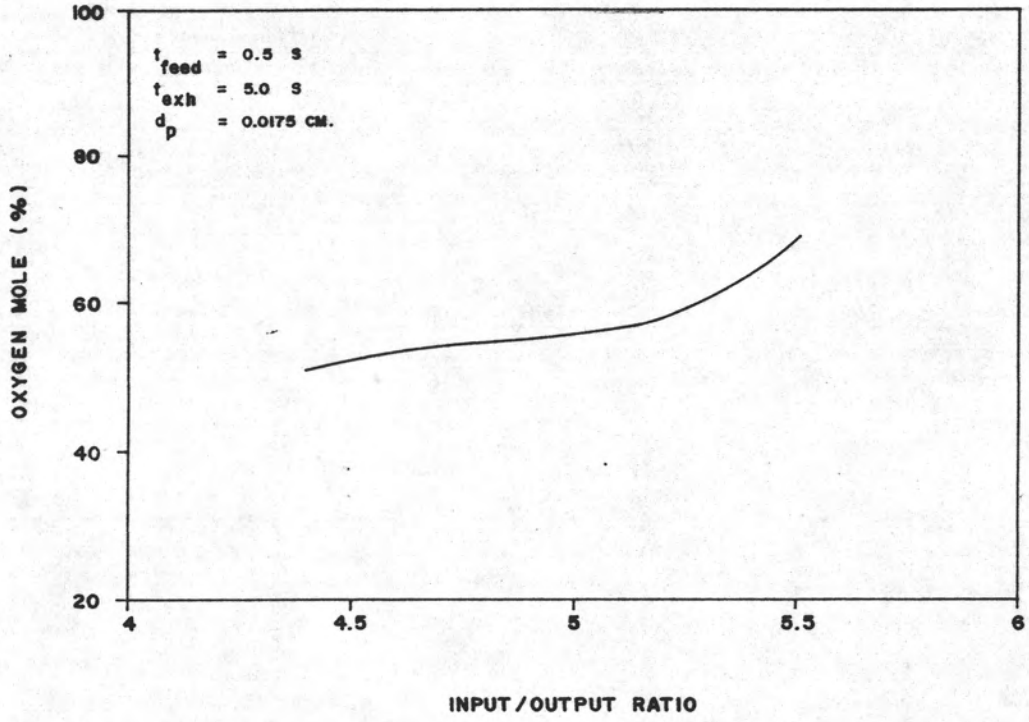

Figure 4.5 Simulation of variation of concentration of oxygen in product stream as a function of input/output ratio in molar terms.

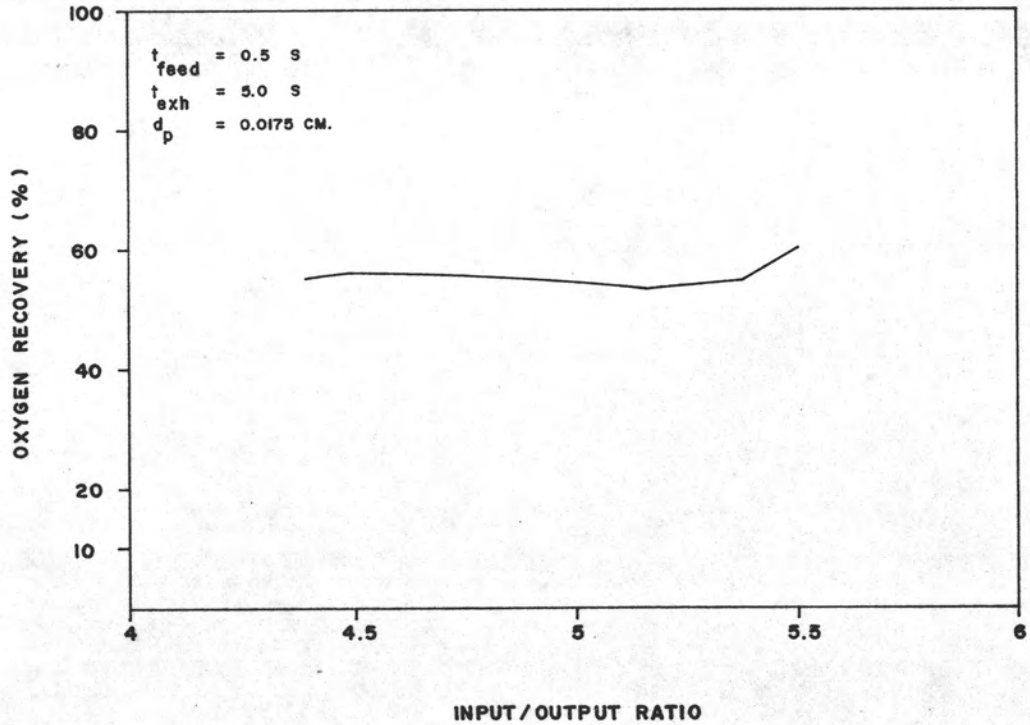

Figure 4.6 Simulation of variation of oxygen recovery (%) as a function of input/output ratio in molar terms.

TABLE 4.1 EFFECT OF MOLAR RATIO VARIATION ON OXYGEN CONCENTRATION FOR SIMULATION

MOLE INPUT (MOLES)	MOLE OUTPUT (MOLES)	INPUT/OUTPUT RATIO	MOLE % O2 IN PRODUCT	OXYGEN RECOVERY (%)
0.363	0.083	4.4	50.9	55.0
0.444	0.099	4.5	52.7	56.0
0.524	0.110	4.8	55.1	55.1
0.598	0.116	5.2	57.4	53.0
0.704	0.127	5.4	63.8	54.8
0.758	0.138	5.5	69.6	60.3

* SIMULATION CONDITION AT FEED TIME = 0.5 SECONDS
EXHAUST TIME = 5 SECONDS AND PARTICLE DIAMETER = 0.0175 CM

TABLE 4.2 EFFECT OF FEED TIME VARIATION ON OXYGEN CONCENTRATION FOR SIMULATION

FEED TIME (SECOND)	MOLE INPUT (MOLES)	MOLE OUTPUT (MOLES)	INPUT/OUTPUT RATIO	MOLE % O2 IN PRODUCT	OXYGEN RECOVERY (%)
0.5	0.766	0.210	3.6	66.5	86.7
0.7	0.713	0.203	3.7	67.6	91.6
1.0	0.761	0.220	3.5	50.1	68.9
1.5	0.807	0.219	3.7	45.5	58.7

* SIMULATION CONDITION AT EXHAUST TIME = 10 SECONDS, PARTICLE DIAMETER = 0.0175 CM
CONSTANT MOLAR FLOW RATE = 0.02 MOLE/S

4.2 Simulation with variation of molar ratios.

Having developed the equations of the model for the pressurization and blowdown step both steps are now put together in a single cycle with the end of one step being the initial conditions of the other step. The cycles are then calculated until steady-state is reached. During the simulation the boundary conditions of this study with V_s taking on a value of 2,250 cm^3 is used . It is to be noted that E is an arbitrarity set value of the exit molar flow rate .

In this simulation case a variation in input/output ratio (moles in product stream on the average /moles in feed stream on the average) for a set of conditions for d_p = 0.0175 cm ,feed time= 0.5 seconds ,exhaust time = 5 seconds .The simulation results obtained are shown in table 4.1 and figures 4.5 and 4.6 . Figure 4.5 indicates that as less product is obtained from the system an increase in oxygen concentration is obtained. This conclusion is not surprising and was to be expected. Figure 4.6 indicates that as less product is obtained oxygen recovery shows a slight increasing trend. The trend here is not clear as the increase is small . In terms of practical applications the oxygen recovery is not economically crucial as the raw material is free.

In this set of simulations it was not possible to increase E beyond a certain value that would make the input/output ratio go beyond 5.5.The reason was that the pressure in the procuct surge tank was too low to sustain E (i.e. pressure in the surge tank was

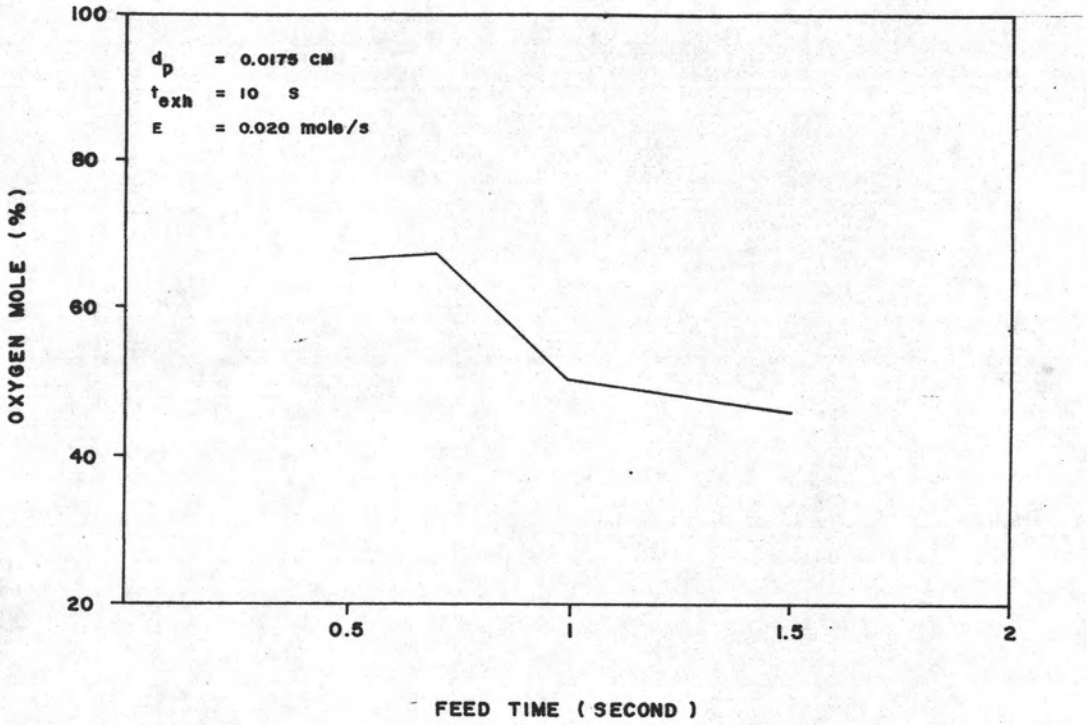

Figure 4.7 Simulation of variation of oxygen concentration in product gas as a function of feed time.

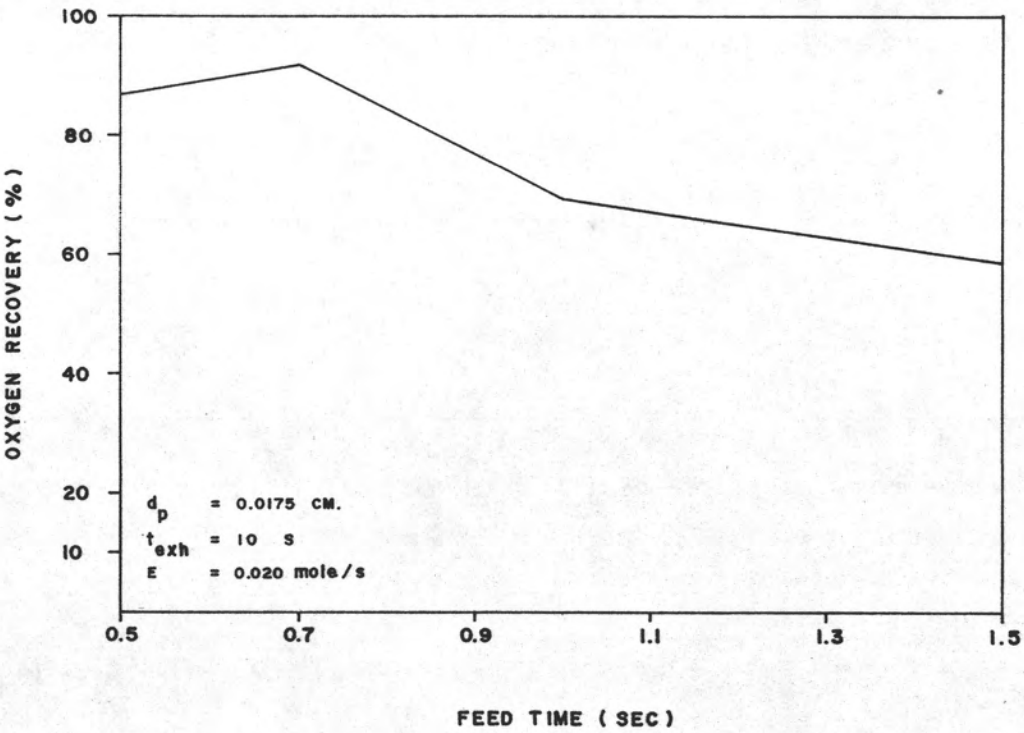

Figure 4.8 Simulation of variation of oxygen recovery (%) as a function of feed time.

TABLE 4.3 EFFECT OF EXHAUST TIME VARIATION ON OXYGEN CONCENTRATION FOR SIMULATION

EXHAUST TIME (SECOND)	MOLE INPUT (MOLES)	MOLE OUTPUT (MOLES)	INPUT/OUTPUT RATIO	MOLE % O2 IN PRODUCT	OXYGEN RECOVERY (%)
5	0.361	0.083	4.4	50.9	55.6
7	0.543	0.120	4.5	57.8	60.8
10	0.764	0.137	5.5	66.3	56.6

* SIMULATION CONDITION AT FEED TIME = 0.5 SECOND, PARTICLE DIAMETER = 0.0175 CM AND CONSTANT MOLAR FLOW RATE = 0.015 MOLE/S

TABLE 4.4 EFFECT OF PARTICLE DIAMETER VARIATION ON OXYGEN CONCENTRATION FOR SIMULATION

PARTICLE DIAMETER (CM)	MOLE INPUT (MOLES)	MOLE OUTPUT (MOLES)	INPUT/OUTPUT RATIO	MOLE % O2 IN PRODUCT	OXYGEN RECOVERY (%)
0.0130	1.230	0.061	20.3	74.6	17.5
0.0140	1.452	0.066	22.0	67.8	14.7
0.0150	1.178	0.066	17.9	65.0	17.3
0.0175	1.918	0.075	12.8	50.9	18.9

* SIMULATION CONDITION AT FEED TIME = 0.5 SECOND, EXHAUST TIME = 5 SECOND PARTICLE DIAMETER = 0.0175 CM AND CONSTANT MOLAR FLOW RATE = 0.012 MOLE/S

less than the outside pressure) and the numerical integration does not converge.

4.3· Simulation of the effect of feed time.

In this case , the feed time is varied for a constant exhaust time of 10 seconds ,a particle diameter of 0.0175 cm and constant molar flow rate (E) of 0.020 mole/s. The resuts obtained from this case shown in table 4.2 and figures 4.7 and 4.8. As shown in figure 4.7 when the feed time is increased the oxygen concentration in the product gas decreases. This result is opposite to what one could expect and that is that large input times should increase product purity . However in the single column PSA the rapid cycles result in pressure gradients that do not have time to equalize but given too long pressurization times the pressure difference between both ends of the column is destroyed. Pressure drop is probably important for the sucessful operation of single column PSA system which requires a careful choice of particle sizes and cycle times to obtain proper dynamic responses with sufficient pressure drops to prevent breakthrough of the more strongly adsorbed species [6]. Short feed times result in high pressure gradients in the bed and ought to be beneficial in terms of oxygen concentration . Therefore an increase in feed time according to the above explanation ought to result in an oxygen concentration decrease. Figure 4.8 shows the oxygen recovery (%) as a function of feed time, which also shows a decrease with increasing feed time which agrees with the trend of figure 4.7 and this was to be expected.

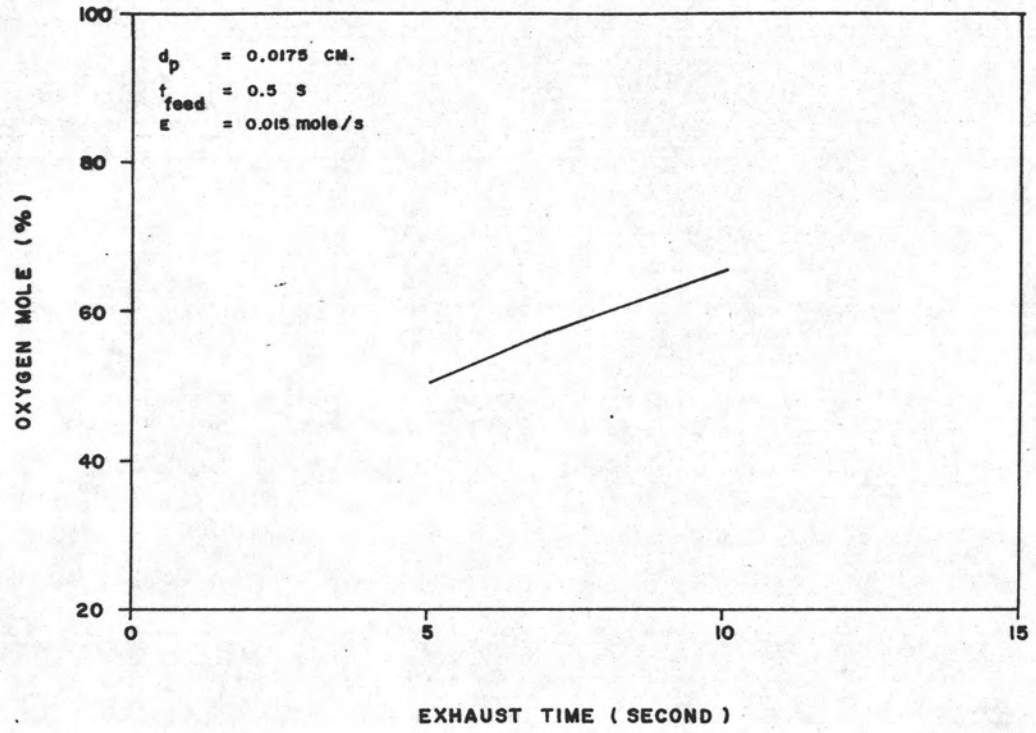

Figure 4.9 Simulation of variation of oxygen concentration in a product gas as a function of exhaust time.

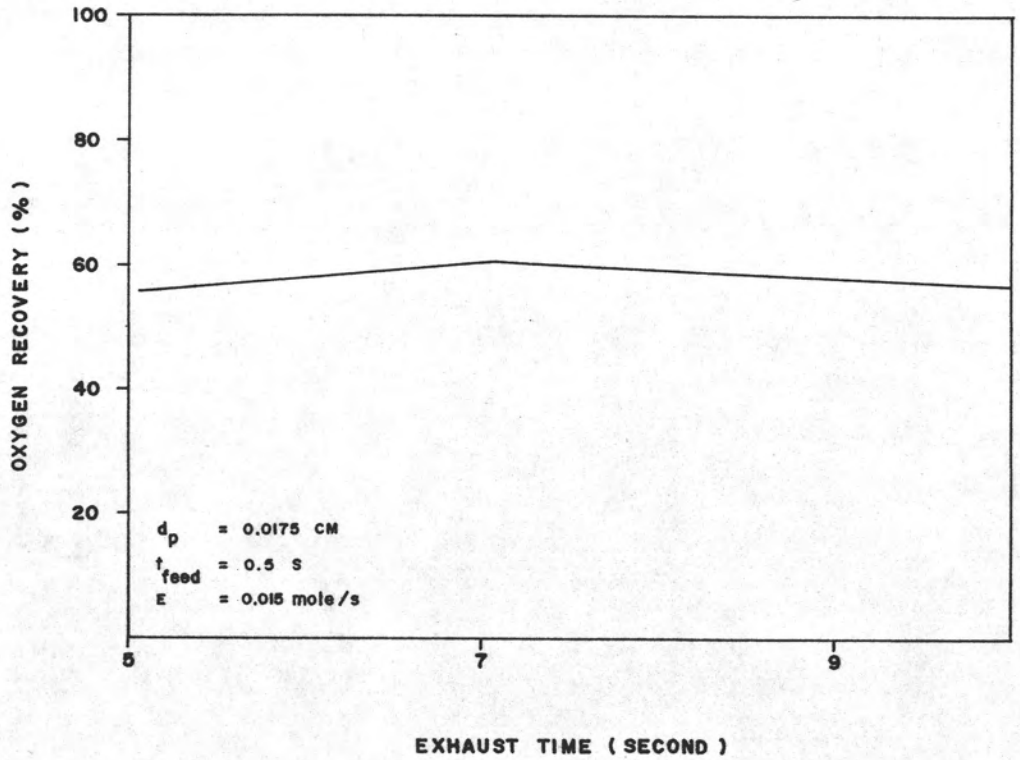

Figure 4.10 Simulation of variation of oxygen recovery (%) as a function of exhaust time.

4.4 Simulation of the effect of exhaust time.

In this case , the effect of exhaust time variation was studied for a constant feed time of 0.5 seconds , a particle diameter of 0.0175 cm and a constant molar flow rate (E) of 0.015 mole /s these variations of exhaust time are shown in table 4.3 and figures 4.9 and 4.10. Increase in exhaust times is shown to result in increased oxygen concentration . The explanation of the behavior may be that increased exhaust times decrease the pressure at the end of the column and promotes high pressure difference between front end of the column for the following pressurization step . Similarly as before this reasoning could explain the increase in oxygen concentration with increased product time. Figure 4.10 shows the oxygen recovery (%) as a function of exhaust time. The result shows an oxygen recovery (%) which varies only slightly when the exhaust time is varied and definite conclusions cannot be drawn.

4.5 Simulation of effect of particle diameter.

As mentioned before that single column PSA requires high pressure gradients in the bed. Therefore one way to produce a pressure drop in the bed is to use small adsorbent particles. As shown in table 4.4 and figure 4.11 as the particle diameters become smaller the concentration of oxygen in the product gas increases. This reinforces the comments made that increased pressure drop in the column increases gas separation.

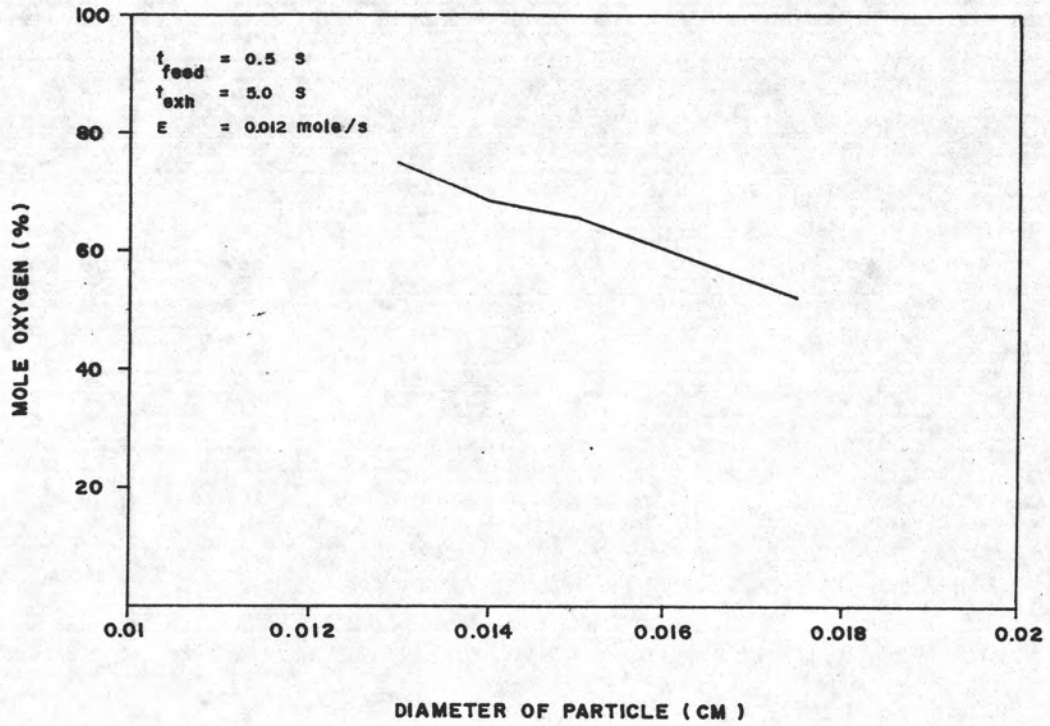

Figure 4.11 Simulation of variation of influence of particle diameter on oxygen concentration of product

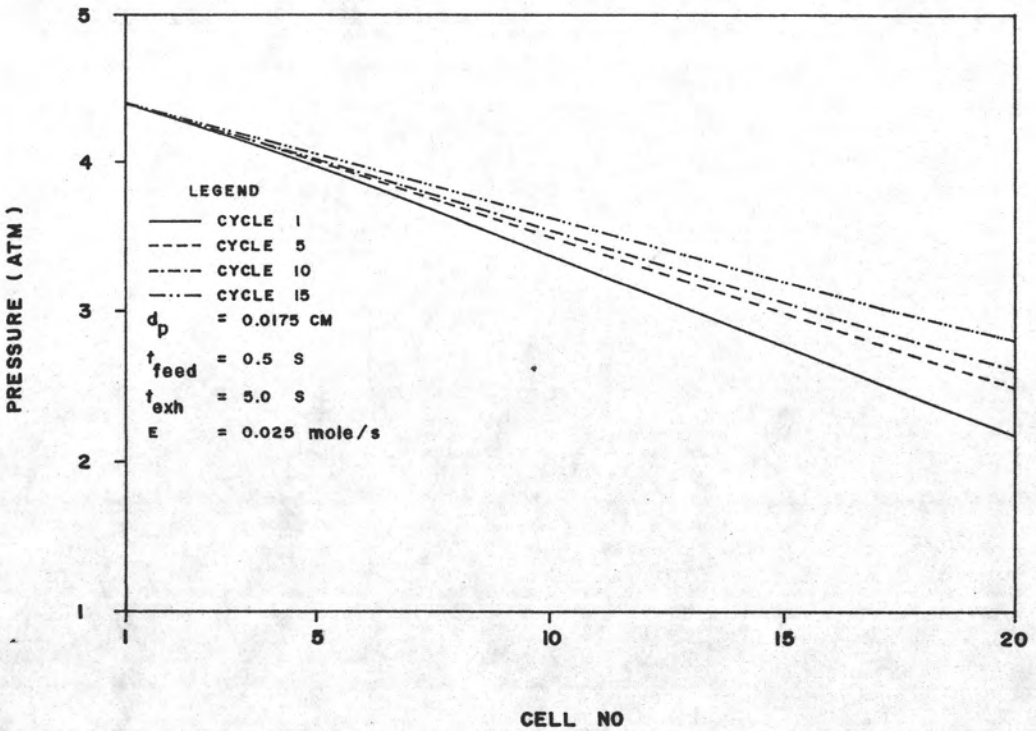

Figure 4.12 Simulation of pressure profile within the adsorber as a function of column length at end of feed time .

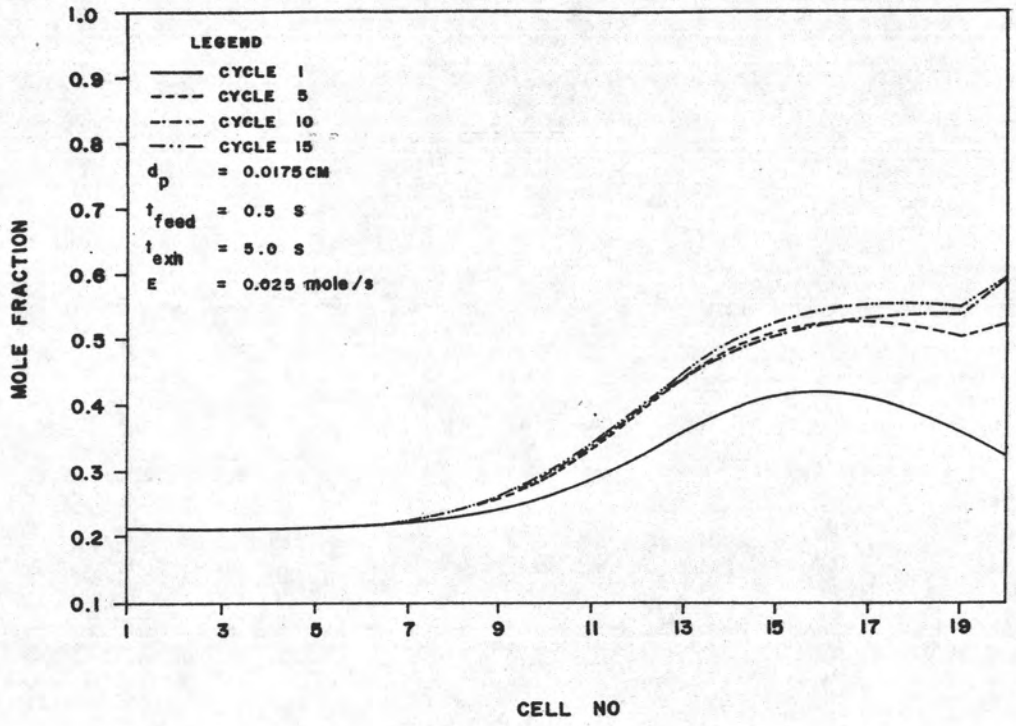

Figure 4.13 Simulation of oxygen concentration profile within the adsorber as a function of column length at end of feed time.

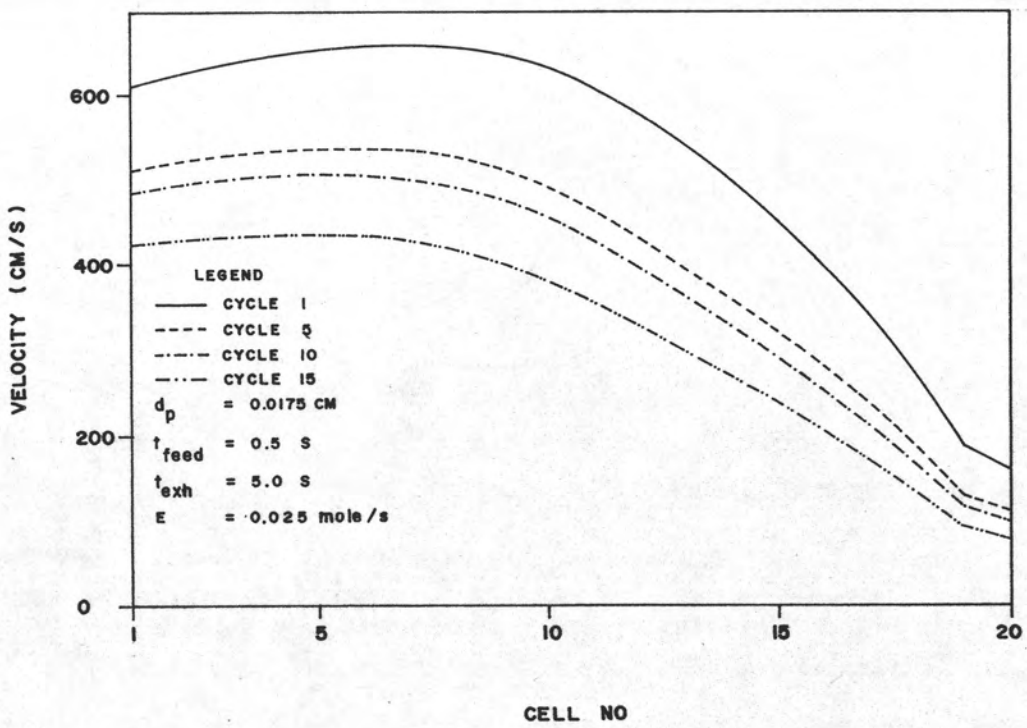

Figure 4.14 Simulation of gas velocity profile within the adsorber as a function of column length at end of feed time .

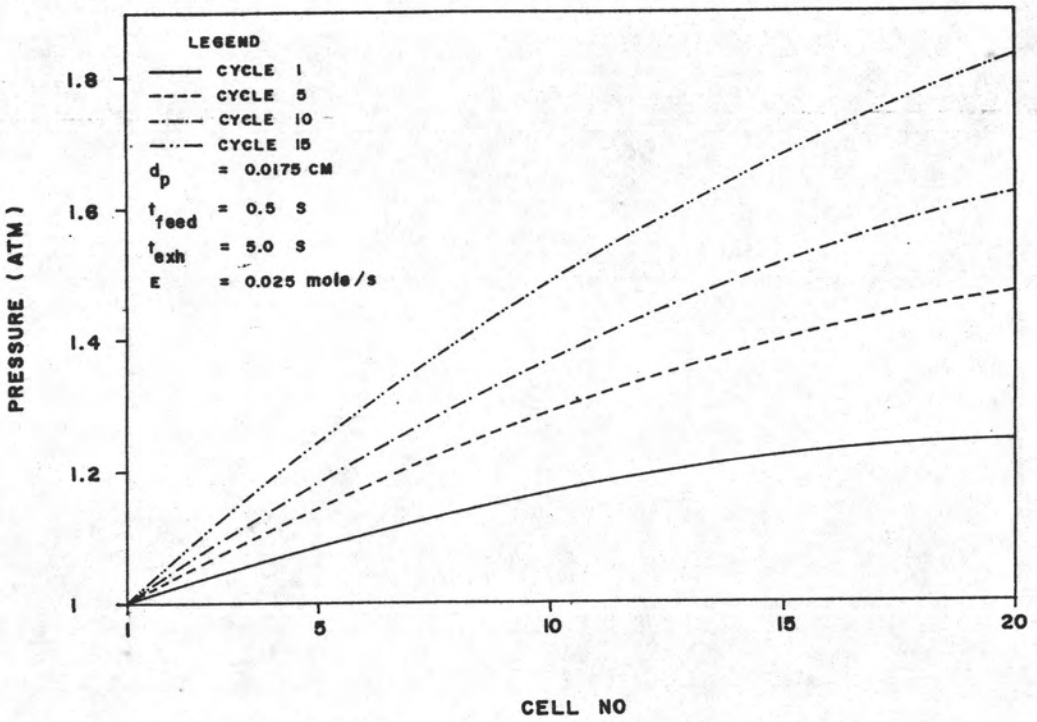

Figure 4.15 Simulation of pressure profile within the adsorber as a function of column length at end of exhaust time .

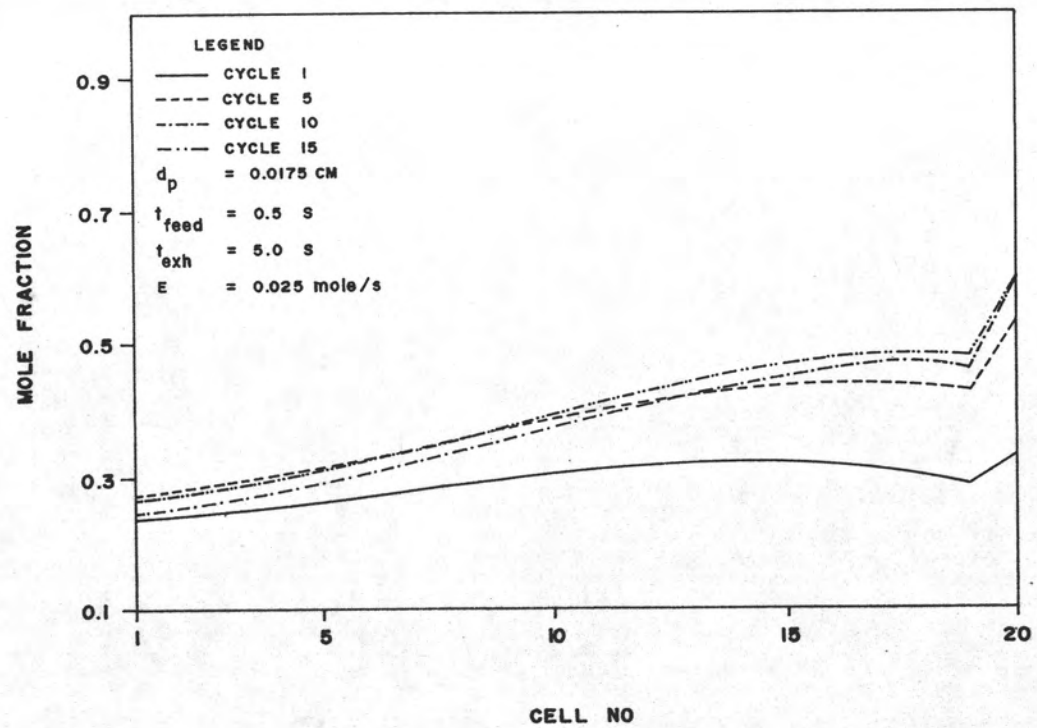

Figure 4.16 Simulation of oxygen concentration profile within the adsorber as a function ofcolumn length at end of exhaust time.

4.6 Pressure , mole fraction and velocity profiles as a function of bed length and cycle time.

This model can predict pressure , mole faction and velocity profiles along the column length at the end of the feed time step and at the end of the exhaust time step. Figures 4.12 - 4.23 refer to one set of simulation for the following conditions : feed time =0.5 seconds, exhaust time = 5 seconds,particle diameter = 0.0175 cm and constant molar flow rate (E) = 0.025mole/s for this simulation steady state is reached after about 15 cycles.

Figure 4.12 shows the pressure profile at the end of the feed time as predicted from this model . The pressure is shown to increase with the number of cycles and there is a permanent pressure drop along the column length within the feed time.

Figure 4.13 shows the oxygen concentration profile at the end of the feed time . Oxygen concentration at the end of the adsorption column is shown to increase with the number of cycles. The oxygen concentration also increases from front end to back-end of column and this trend is absolutely necessary if oxygen concentration is to be increased in the product stream. A discontinuity in the slope of the oxygen mole fraction profile at the back-end of the column is observed , indicating a need for a re-evaluation of the boundary conditions at the back-end of the column or a need to increase the number of discretizatious along the column.

Figure 4.14 shows velocity profiles at the end of the feed time . An increase cycle time results in decreased velocity as the column is filled and this is to be expected. The back-end of the column also has a lower velocity than the front end as the column is being filled and this is also to be expected.

Figure 4.15 shows pressure profiles at the end of the exhaust time steps. Increase in cycle time result in general increase in pressure. This agree with the trend of the pressure profiles during feed time for each cycle where pressures increase with time at the end of feed time . At the end of the column (cell no = 20) the pressure is higher than at the front end of column . This is caused by reduction of pressure in the column down to ambient (atmospheric) pressure and then existence of a product surge tank which purges the column during blowdown.

Figure 4.16 shows oxygen concentration profiles at the end of the exhaust time for various cycles . The results obtained indicate that an increase in number of cycles result in an increase in oxygen concentration with time. This is caused by the purging action with oxygen rich product in the product surge tank. Therefore oxygen concentration increase with time and oxygen concentration increase along the bed length agrees with expected trends . During depressurization nitrogen gas should desorb as an oxygen rich gas purges the column, this is another reason why oxygen concentration increases with cycle time.

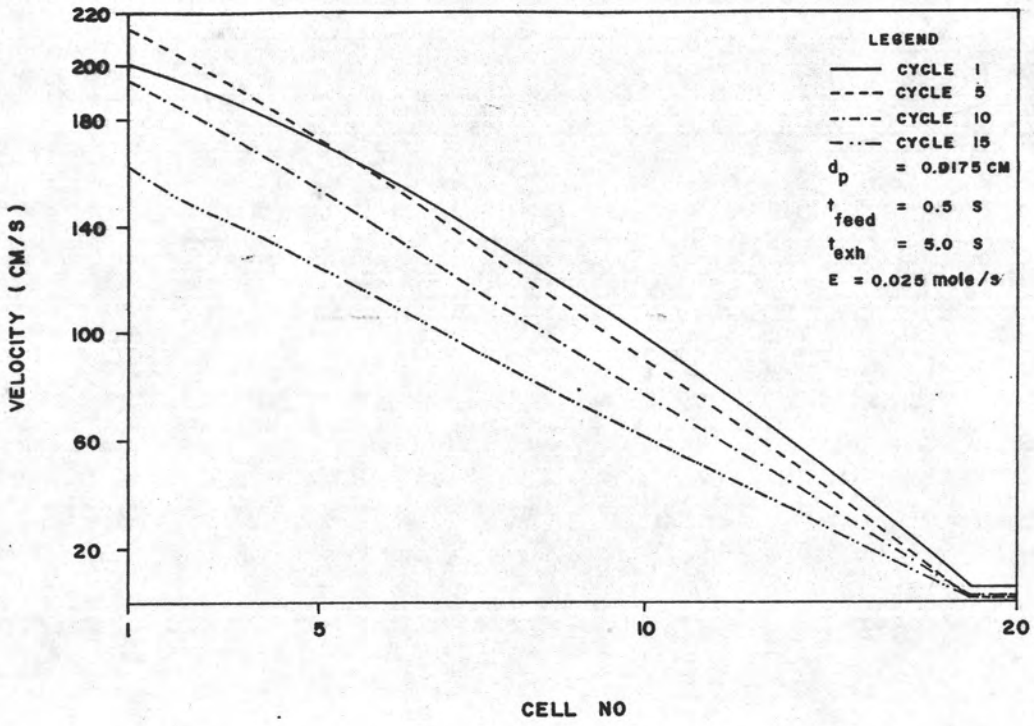

Figure 4.17 Simulation of gas velocity profile within the adsorber as a function of column length at end of exhaust time .

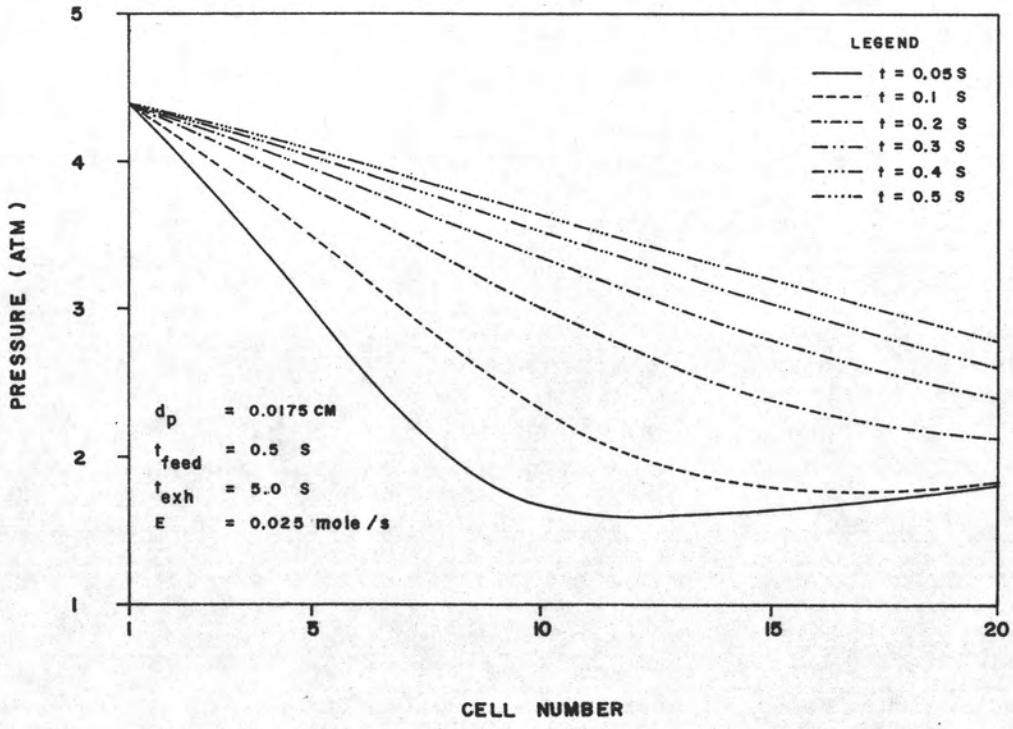

Figure 4.18 Simulation of pressure profile within the adsorber as a function of column length during feed gas time.

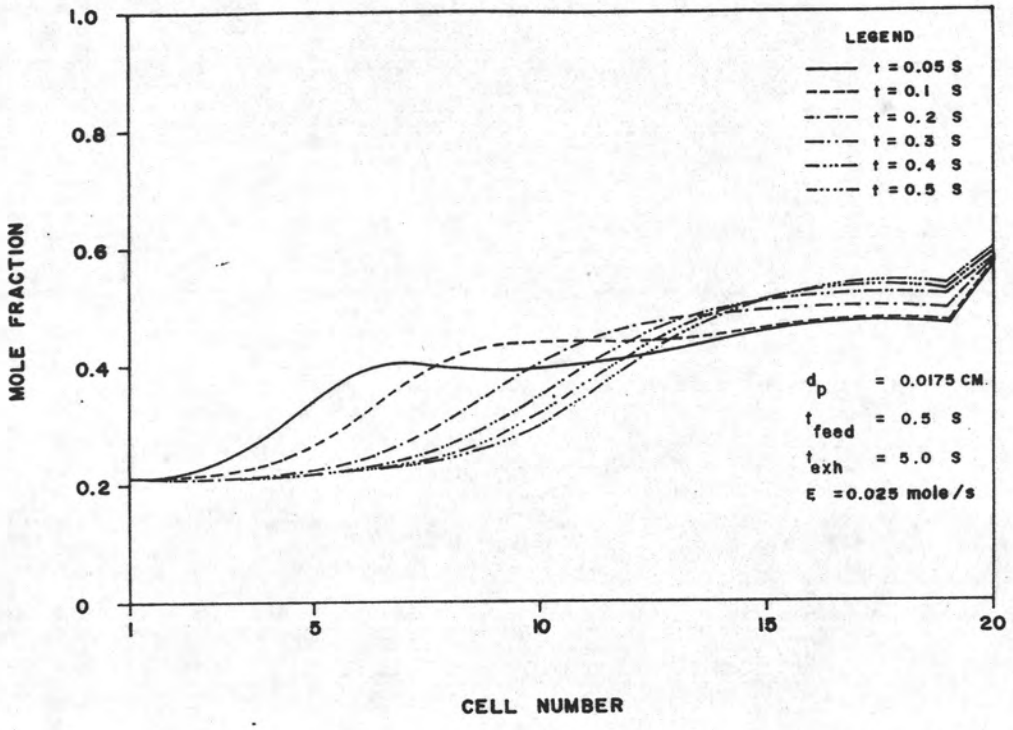

Figure 4.19 Simulation of oxygen concentration profile within the adsorber as a function of column length during feed gas time

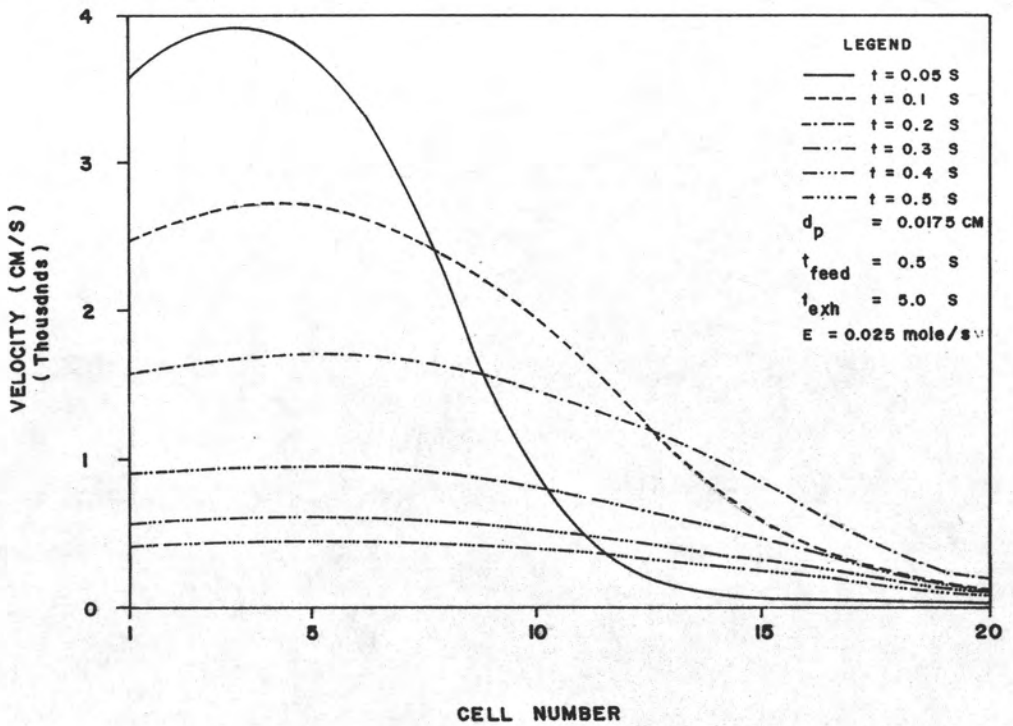

Figure 4.20 Simulation of velocity profile within the adsorber as a function of column length during feed gas time.

Figure 4.17 shows the velocity profile at the end of the exhaust time for various cycles. As expected the velocities decrease with bed length. The velocities also generally decrease with the number of cycles.

The general trends of the profiles for pressure, concentration and velocities obtained through the simulation conform to the trends expected. Figure 4.18 shows the pressure profile within the adsorber as a function of column length during feed time . The pressure increases with increased time and within the set feed time there exits a pressure drop along column length. This curve points to the fact that an excessively long feed time would indeed destroy the pressure drop along the bed.

Figure 4.19 shows the oxygen concentration profile within the adsorber as a function of column length during feed time . When time increases the oxygen concentration profile increases from front to back-end of column. However a discontinuity in the slope of the oxygen concentration curve at the back-end of column was found , indicating a need for a re-evaluation of the boundary condition at the end of the column.

Figure 4.20 shows the velocity profile within the adsorber as a function of column length during feed time . When time increases the velocity levels decrease. This is to be expected as the adsorption column is being filled and the adsorbent is being saturated with gas.

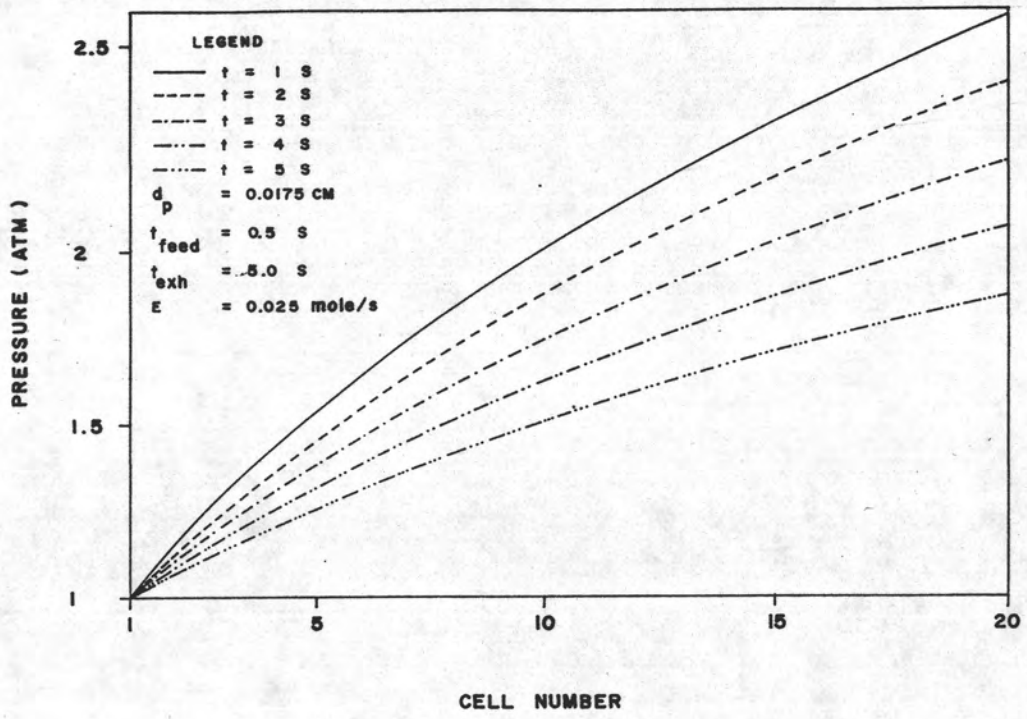

Figure 4.21 Simulation of pressure profile within the adsorber as a function of column length during exhaust gas time.

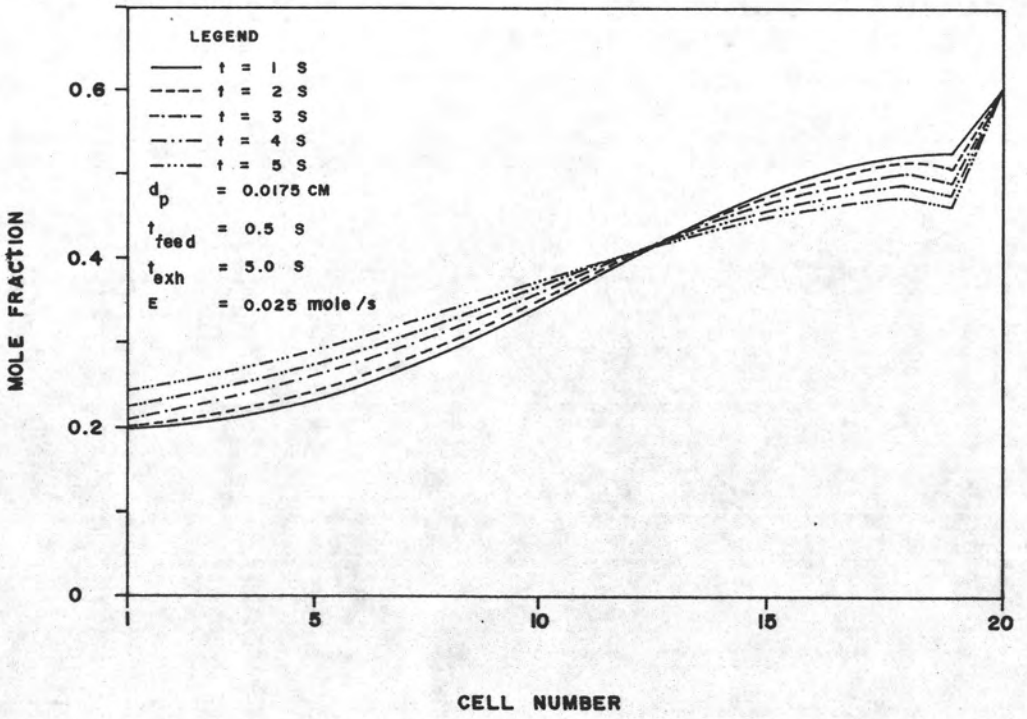

Figure 4.22 Simulation of oxygen concentration profile within the adsorber as a function of column length during exhaust gas time.

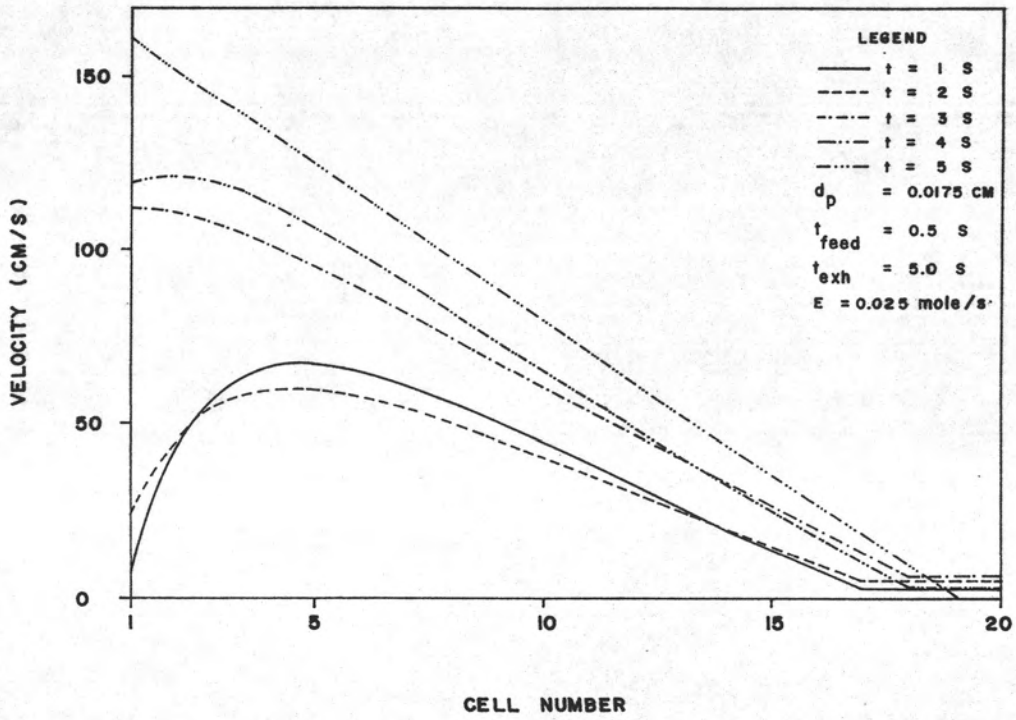

Figure 4.23 Simulation of velocity profile within the adsorber as a function of column length during exhaust gas time.

Figure 4.21 shows pressure profiles within the adsorber as a function of column length during exhaust time . Increase in time results in decreased pressure profiles. This behavior is likewise expected when the front-end of the column is open to the atmospheric pressure during exhaust time.

Figure 4.22 shows the oxygen concentration profile within the adsorber as a function of column length during exhaust time. It is to be noted in this figure that the oxygen concentration at the back-end has a constant value which corresponds to the concentration of oxygen in the product surge tank. However the profiles are generally similar. One comment to be made is the discontinuity at the back-end of the column which calls for a re-evaluation of the boundary conditions.

Figure 4.23 shows the velocity profile within the adsorber as a function of column length during exhaust time . Increase in time results in increased velocity profiles. This behavior is caused by a relation between mole fraction and pressure in equation 3.27 which was used to calculate velocity. As seen in equation 3.27 velocity is proportional to pressure and inversely proportion to mole fraction and result in increased velocity when time increases. This however is yet to be confirmed experimentally.